Ultraviolet and solar-blind spectral imaging with subwavelength transmission gratings

S. H. Lim and E. T. Yu[a]

Department of Electrical and Computer Engineering, University of California, San Diego La Jolla, California 92093-0407, USA

Aluminum gratings with subwavelength slit widths were designed and analyzed for spectral filtering of ultraviolet (UV) light. Although schemes for optical wavelength filtering have been thoroughly studied, options for UV wavelength filtering are far more limited. We analyze the unique requirements for UV based imaging and evaluate the suitability of our structures by electromagnetic simulations and experimental measurements. Rayleigh–Wood anomalies are shown to lead to sharp drops in transmission at resonance wavelengths, producing a high finesse band reject filter. Finally, we show that the structures are effective for both TE and TM polarizations and easily integrated onto semiconductor photodetectors. © 2009 American Institute of Physics. [doi:10.1063/1.3257365]

Recent advances in high quantum efficiency AlGaN based photodetectors[1–4] have made possible solid state focal plane array imaging for near ultraviolet (300–400 nm) and solar-blind (<280 nm) wavelengths. For spectrally resolved imaging, filtering structures will have to be integrated on top of the pixel array. While effective filtering schemes[5] compatible with very large scale integrated circuit exist for optical array imagers, the materials typically used for such structures such as dichroic mirrors are generally not suitable for ultraviolet (UV) wavelengths due to high absorption. In addition, designing solar-blind filters[6–8] is generally regarded as particularly challenging[6] because of the lack of high quality optical materials in this wavelength range. A survey of commercially available discrete solar-blind filters shows that such filters have a full width at half maximum of about 20 nm or less. This is sensible as the practically detectable solar-blind wavelength range is somewhat narrow (200–280 nm). Thus, in a four color imaging scheme, for example, this region of the electromagnetic spectrum would have to be split into 20 nm wavelength slices.

We demonstrate here a UV wavelength filtering scheme that makes use of metallic gratings with subwavelength slit sizes ($\lambda/3 \sim \lambda/4$) and materials compatible with UV operation. A variety of subwavelength metallic structures have been the subject of intense study,[9–13] particularly with regard to the extraordinary transmission effect found in periodic hole arrays on metallic thin films.[10] The resonant excitation of a surface plasmon (SP) on one side of the metal-dielectric interface followed by coupling through very small ($\sim\lambda/10$) holes to another SP on the reverse side was found to lead to unexpectedly high transmission of light, leading to potential applications for optical filtering. In contrast to this approach, we exploit here the effect of reduced transmission at the Rayleigh–Wood anomaly,[14] found in metallic gratings with relatively wide slits. Although the Rayleigh–Wood anomaly is usually associated with the resonant excitation of an SP, the same effect is also present whenever there exists a surface mode, such as a slab waveguide mode in close proximity to the grating.[5]

To illustrate the basic concept, we first simulate the transmission grating structure shown in Fig. 1(a), consisting of a 50 nm thick, 450 nm period, and 150 nm slit width Al grating on top of silica designed for filtering in the TM mode. We simulate the transmission of light through this structure using a finite element method program.[15] To best demonstrate the excitation of an SP mode at 340 nm, which occurs at the silica/Al boundary, we illuminate the structure from the silica side. As indicated in Fig. 1(b), each dip in the transmission spectrum, shown in Fig. 1(c), is associated with a resonant excitation of an SP mode, given by the Bragg diffraction condition,

$$k_{SP}(\omega) = k_{\parallel} + m \cdot 2\pi n/l, \tag{1}$$

where k_{SP} is the wavevector of an SP mode on either the air or the glass side, $k_{\parallel}$ is the wavevector of the incident light parallel to the grating surface, m is the diffraction order $(1, 2, 3\ldots)$, n is the index of refraction of the dielectric boundary, and l is the grating period. For normally incident
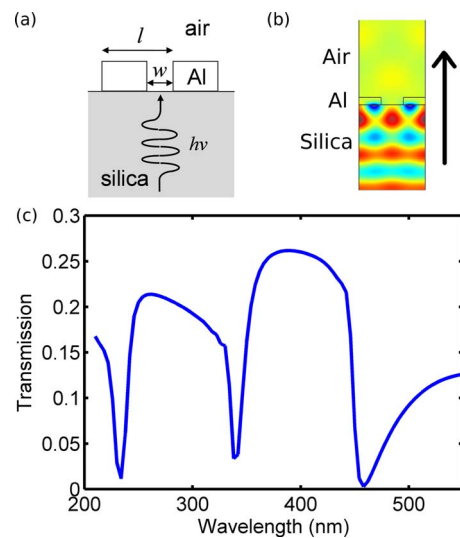

FIG. 1. (Color online) (a) Schematic of 50 nm thick aluminum grating deposited on fused silica substrate. (b) Simulation of transverse magnetic field profile shown at resonance (340 nm) for l=450 nm and w=150 nm. (c) Corresponding simulated TM transmission spectrum.

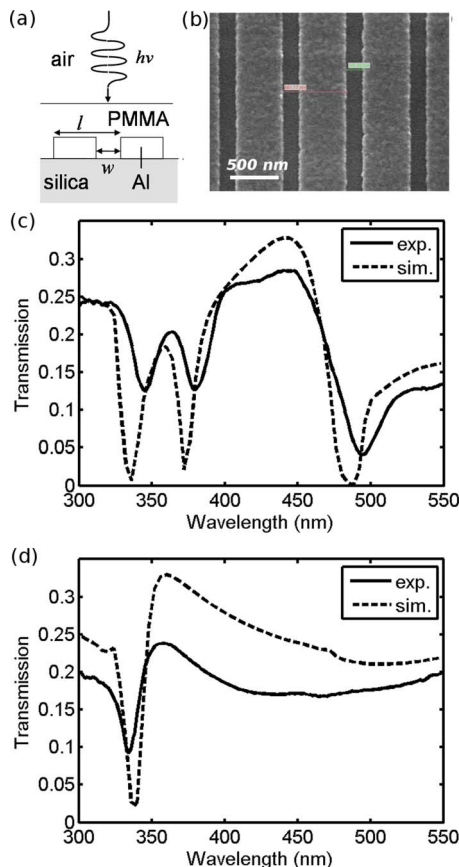[a]Electronic mail: ety@ece.utexas.edu.

FIG. 2. (Color online) a) Schematic of 50 nm thick Al grating deposited on fused silica with PMMA spin-coated overlayer. (b) SEM image of the completed grating structure with $l=650$ nm and $w=150$ nm. (c) Simulated (dashed line) and measured (solid line) TM transmission spectra of the structure in (a) with 225 nm of PMMA over the Al grating with $l=650$ nm and $w=150$ nm. (d) Simulated (dashed line) and measured (solid line) TE transmission spectra of the same structure, but with 80 nm of PMMA over the Al grating.

light, which we will assume from here onwards, $k_{\parallel}=0$. We see that the dip at 450 nm is due to first order diffraction $(m=1)$ into an SP mode at the air/Al interface, while the dips at 340 and 230 nm are due the second and third order $(m=2,3)$ diffraction into SP modes at the silica/Al interface. We note that for higher-order diffraction $(m>1)$, the width of the resonances is on the order of 10–20 nm, and therefore satisfies the operational goal for solar-blind applications.

We note also that the use of aluminum as a plasmonic material is crucial for realizing such structures with acceptable loss and line width broadening. Traditional materials such as gold and silver are too lossy in the UV wavelengths. Further analysis shows that the most important criterion for choosing a metal is the reflectivity. A survey of a broad range of metals shows that Aluminum is by far the best in terms of reflectivity due to its large negative dielectric function, followed by indium and then tin. However, aluminum is easily oxidized in air and must be protected by dielectric coatings to preserve the reflectivity of the metal.

For experimental verification and analysis of these behaviors, Aluminum transmission grating structures were fabricated on fused silica substrates, as shown in Fig. 2(a) and 2(b), with the goal of measuring the Rayleigh–Wood anomaly resonances in the near UV wavelengths. 650 nm period gratings with 150 nm slit widths were patterned using

electron beam lithography and e-beam evaporation of aluminum (50 nm) followed by liftoff with acetone. A 225 nm polymethyl methacrylate (PMMA) layer was coated over the grating and baked at 180 °C for 1.5 min to protect it from oxidation. The refractive index of PMMA as published by MicroChem Corp.[16] varies from 1.55 at 300 nm to 1.48 at 900 nm. In our simulations, we use a constant refractive index of 1.49. Transmission measurements were obtained using a monochromator fed by a xenon arc lamp as a broadband UV source. Monochromatic UV light from the output is passed through a light chopper followed by an α-BBO Glan–Thompson polarizer and focused onto the sample surface. Light transmitted through the sample is detected by a GaP photodiode and the signal is fed into a Lock-in amplifier. Additional details on the simulation and measurement configuration have been described elsewhere.[15]

Figure 2(c) shows the simulated and measured TM transmission spectra for this structure, which are in good agreement. The dips at 340 and 500 nm are due to third and second order diffraction into an SP mode, respectively. The dip at 380 nm is not due to an SP mode because it is far from any resonance condition predicted by Eq. (1). In fact, the simulation shows that this resonance is due to a second order diffraction into a TM slab waveguide mode in the PMMA layer above the grating.

The presence of a slab waveguide above the grating is particularly beneficial for TE polarized light because SP modes do not exist for TE polarization. We therefore perform the same experiment for TE polarized light using the same structure as before but with an 80 nm PMMA layer. Figure 2(d) shows the measured and simulated TE transmission spectrum for this structure. The dip at 340 nm is due to a second order diffraction into a TE slab waveguide mode.

The existence of TE resonances due to the PMMA waveguiding layer suggest an interesting possibility for designing polarization independent transmission grating filters. The TM resonances due to SP modes are mostly confined to the surface of the grating due to the exponential decay of the electromagnetic fields away from the metallic surface. Therefore, the dispersion of the SP mode should be insensitive to the thickness of the dielectric waveguiding layer, provided that the air/dielectric boundary is sufficiently far from the metal/dielectric boundary. For the TE mode however, the thickness of the dielectric layer naturally has a strong effect on the dispersion of the waveguide mode. Therefore, by tuning the thickness of the waveguide, one can shift the TE resonance without affecting the TM resonance, thus raising the possibility of designing structures where the TM and TE resonances occur at the same wavelength, allowing polarization insensitive wavelength filtering.

Furthermore, the grating structures presented here can be directly integrated onto a semiconductor substrate as a Schottky contact, thus forming a Schottky photodiode. To demonstrate such a configuration, we designed and fabricated a filter/Schottky contact bimetallic grating on an n/n + epitaxial Si wafer, shown in Fig. 3(a). The donor concentration of the expitaxial layer is $(0.5-1) \times 10^{15}$ cm^{-3} and the thickness is 4.5–5.5 μm. The grating has a period of 550 nm and slit width of 180 nm, and consists of 15 nm of gold and 45 nm of aluminum. The gold layer forms the Schottky contact with the Si epilayer while the aluminum layer on top forms the interface supporting the SP mode with air.
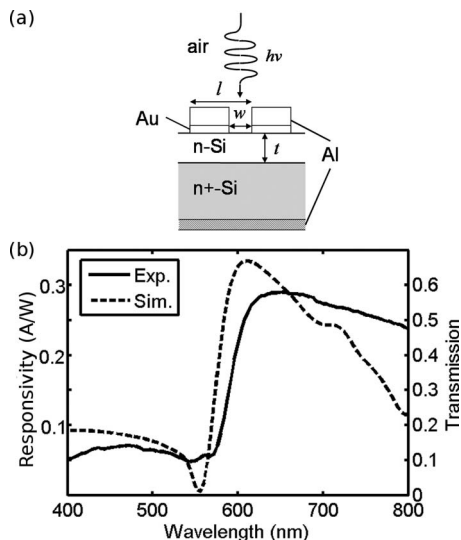
(a)

(b)

FIG. 3. (a) Schematic of 15 nm Au/45 nm Al bimetallic grating on Si epitaxial wafer with $l=550$ nm, $w=180$ nm, and $t\sim5$ μm. (b) Simulated transmission spectrum (dashed line) and measured photoresponsivity (solid line) of the grating structure integrated atop an n/n+Si wafer forming a Schottky photodiode.

Our simulations, shown in Fig. 3(b), reveal that near 550 nm, there is a strong drop in transmission into the Si substrate due to the first order diffraction into an Al/air SP mode. For the experimental demonstration, we measure the photocurrent directly from the Schottky photodiode using the same apparatus described previously, except with the light source replaced by a quartz tungsten halogen lamp. The result, shown in Fig. 3(b), confirms that at around 550 nm, there is a sharp drop-off in responsivity with decreasing wavelength, in accordance with the strong drop in transmission at around the same wavelength as predicted by the transmission simulation. The dip in the responsivity measurement is not as pronounced as the dip in the transmission simulation, suggesting a broadened resonance. This could be due to oxidation effects as well as a slightly off-normal angle of incidence for the incident light relative to the plane of the device.

In summary, we have studied Rayleigh–Wood anomaly based resonant structures with Aluminum gratings for UV spectrally resolved imaging on integrated photodetectors. The structures were shown to possess good transmission and wavelength selectivity extending through the solar-blind wavelength range. Experimental verification of the concept was carried out in the near UV and visible wavelengths. Also, integration of such structures on a semiconductor photodiode was demonstrated and tested on Si Schottky photodiodes. The dual functionality of such structures as an optical filter and Schottky contact has obvious advantages in terms of processing. Finally, we suggest that polarization independent structures can be realized by careful tuning of the dimensional parameters.

[1]N. Biyikli, O. Aytur, I. Kimukin, T. Tut, and E. Ozbay, Appl. Phys. Lett. **81**, 3272 (2002).

[2]E. Ozbay, N. Biyikli, I. Kimukin, T. Kartaloglu, T. Tut, and O. Aytur, IEEE J. Sel. Top. Quantum Electron. **10**, 742 (2004).

[3]D. Walker, X. Zhang, P. Kung, A. Saxler, S. Javadpour, J. Xu, and M. Razeghi, Appl. Phys. Lett. **68**, 2100 (1996).

[4]E. J. Tarsa, P. Kozodoy, J. Ibbetson, B. P. Keller, G. Parish, and U. Mishra, Appl. Phys. Lett. **77**, 316 (2000).

[5]S. Hernandez, O. Bouchard, E. Scheid, E. Daran, L. Jalabert, P. Arguel, S. Bonnefont, O. Gauthier-Lafaye, and F. Lozes-Dupuy, Microelectron. Eng. **84**, 673 (2007).

[6]I. Avrutsky and V. Kochergin, Appl. Phys. Lett. **82**, 3590 (2003).

[7]V. Kochergin, M. Christophersen, and P. R. Swinehart, Proc. SPIE **5554**, 223 (2004).

[8]J. Y. Duboz, N. Grandjean, A. Dussaigne, M. Mosca, J. L. Reverchon, P. G. Verly, and R. H. Simpson, Eur. Phys. J.: Appl. Phys. **33**, 5 (2006).

[9]P. B. Catrysse and S. Fan, J. Nanophotonics **2**, 021790 (2008).

[10]T. W. Ebbesen, H. J. Lezec, H. F. Ghaemi, T. Thio, and P. A. Wolff, Nature (London) **391**, 667 (1998).

[11]A. Hessel and A. A. Oliner, Appl. Opt. **4**, 1275 (1965).

[12]D. C. Skigin and R. A. Depine, Phys. Rev. E **74**, 046606 (2006).

[13]K. G. Lee and Q. H. Park, Phys. Rev. Lett. **95**, 103902 (2005).

[14]H. Lochbihler, Phys. Rev. B **50**, 4795 (1994).

[15]S. H. Lim, W. Mar, P. Matheu, D. Derkacs, and E. T. Yu, J. Appl. Phys. **101**, 104309 (2007).

[16]R. Hardman, personal communication (11 June 2009).